Molecular Crystals and Liquid Crystals
Publication details, including instructions for authors and subscription information:
http://www.tandfonline.com/loi/gmcl16

Ultrasonic Imaging Utilizing a Nematic Liquid Crystal

S. Nagai [a] & K. Iizuka [a]
[a] National Research Laboratory of Meteorology, 1-10-4, Kaga, Itabashi, Tokyo, Japan
Version of record first published: 18 Oct 2010.

To cite this article: S. Nagai & K. Iizuka (1978): Ultrasonic Imaging Utilizing a Nematic Liquid Crystal, Molecular Crystals and Liquid Crystals, 45:1-2, 83-101

To link to this article: http://dx.doi.org/10.1080/00268947808084995

Mol. Cryst. Liq. Cryst., 1978, Vol. 45, pp. 83–101

Printed in Holland

Ultrasonic Imaging Utilizing a Nematic Liquid Crystal

S. NAGAI and K. IIZUKA

National Research Laboratory of Meteorology
1-10-4, Kaga, Itabashi, Tokyo, Japan

(*Received June 15, 1977; in final form August 23, 1977*)

Acousto-optical (birefringence) effect in a homeotropically aligned dielectric-positive material *p-n*-pentyl *p'*-cyanobiphenyl has been investigated. A new liquid crystal image converter is developed. In order to improve the resolution, a liquid crystal cell is divided into small arrays, which restrict orienting action of the ultrasound in small regions. Amelioration in the decay time is also made applying a reorienting electric field.

The results are successfully interpreted within the framework of our previous model based on the acoustic streaming effect.

INTRODUCTION

Ultrasonic imaging through nematic liquid crystals is an attractive subject to study. Kessler and Sawyer[1] showed acoustically excited dynamic scattering. Mailer *et al.*[2] demonstrated the birefringence effect in homeotropic texture. Greguss[3,4] uses them as "acoustical-to-optical converter cell." Nevertheless the image quality is, at present, not satisfactory.

The properties of liquid crystals have not been extensively capitalized for the ultrasonic display. Liquid crystals still remain a candidate for this purpose. This is because of the fact that the orienting action of the ultrasound are not completely understood. In a previous paper,[5] one of the authors has proposed a new mechanism which involves the acoustic streaming and suggested a scheme to improve a liquid crystal detector as follows:

1) Resolution could be improved by dividing a cell into a matrix of liquid crystal arrays, which localize the acoustic streaming.

2) A pulse mode operation of the ultrasound together with the application of an electric field is desirable to reduce the response time. In this case a dielectric-positive material should be used.

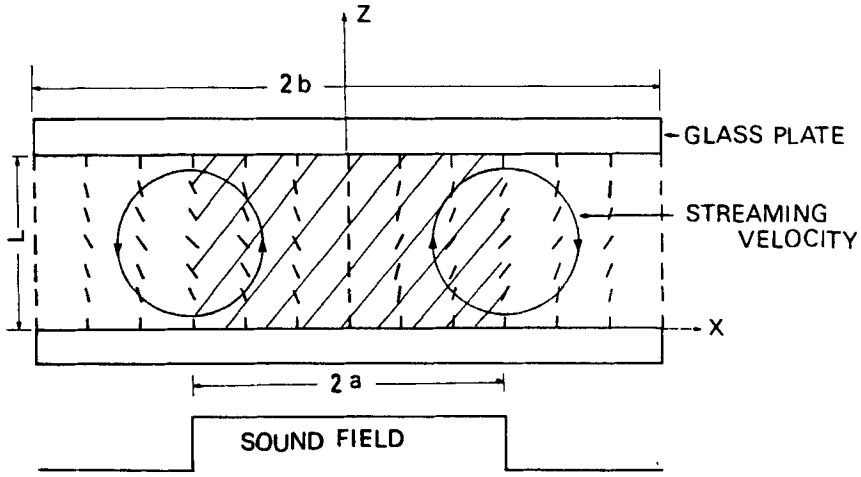

FIGURE 1 Acoustic streaming effect. Small bars express liquid crystal molecules.

Schematic drawing of the acoustic streaming effect is shown in Figure 1. The velocity gradient parallel to the boundary wall leads to deformation of the initial orientation. Since the acoustic streaming penetrates into non-irradiated region, ultrasonic images are smeared out.

The present paper deals with a further study of acousto-optical (birefringence) effect of liquid crystals. In Section 2 we report measurements of the birefringence effect on a dielectric-positive material PCB (*p-n*-pentyl *p'*-cyanobiphenyl) caused by the ultrasound. In Section 3 a liquid crystal image converter is described and in Section 4 the obtained results are discussed within the framework of the model on the acoustic streaming effect.

1 EXPERIMENTAL

The investigated PCB sample was purchased from BDH Co. and used without further purification. The liquid crystal cell consisted of a thin layer of PCB (100 μm) sandwiched between two transparent glass plates (2 cm sq. 130 μm thick), separated by a polyester spacer. Transparent electrodes of indium oxide were used in the case of voltage application. Homeotropic texture was achieved by coating the glass surfaces with lecithin.

The liquid crystal cell was immersed in a water bath and put 25 cm apart from a PZT transducer (diameter 50 mm). Three transducers were used. One was driven at 0.9 and 3.2 MHz. The others were used at 2.1 and 6.0 MHz respectively. A He–Ne laser was used as monochromatic light source. The

cell was placed between crossed polarizers, perpendicularly to light beam. Optical measurements were carried out at several ultrasonic incident angles. At oblique incidence, light transmission was measured and at normal incidence, light reflection as a function of the acoustic intensity. The acoustic intensity at the same position as the liquid crystal cell is placed was measured in water by means of a torsion pendulum. A detailed experimental technique is described in the earlier paper.[5] All measurements were performed at $20 \pm 1°C$ except those for the discussion of temperature dependence.

2 BIREFRIGENCE EFFECT OF PCB

Figure 2 represents the variation in the optical transmission as a function of the acoustic intensity for different frequencies. The normal of the cell was making an angle of 20° with respect to the ultrasonic beam in order to avoid multiple reflection between the transducer and the cell. The optical transmission occurs about 5 mW/cm^2 and reaches a maximum value over 100 mW/cm^2. In comparison with MBBA (*p*-*n*-methoxybenzylidene *p'*-*n*-butylaniline), PCB is a little more sensitive to the ultrasound.

Although the acousto-optical effect at 6 MHz is the most remarkable in Figure 2, it is considerably angle-dependent. The angular dependence is indicated in Figure 3. As the ultrasonic frequency increases, the angular dependence becomes complex. It can be seen that over the whole incident angle the cell is more birefringent at 1 and 2 MHz. The ultrasound at 3 MHz is less effective. At 6 MHz the sensitivity decreases rapidly at higher incident angles. As an image converter, the use of high frequency is desirable in view of the resolution. Consequently we used the ultrasound of 2.1 MHz in the following experiments.

The temperature dependence of optical transmission is presented in Figure 4. The sensitivity increases with increasing temperature. However in the vicinity of the nematic-isotropic transition temperature, the fluctuation of molecular orientation grows and it becomes difficult to maintain a uniform homeotropic orientation in a large area.

The response time is shown in Figure 5. The decay time is greater than the rise time. So the former determines the overall performance time. As PCB is a dielectric-positive material, molecules will restore to homeotropic texture applying an electric field. Figure 6 shows the voltage dependence of the decay time under the electric field. It reduces with increasing the applied voltage, as expected. In the present study an A.C. voltage (100 Hz) was used to avoid charge injection from the electrodes. The effect of electric field was constant up to about 2 KHz.

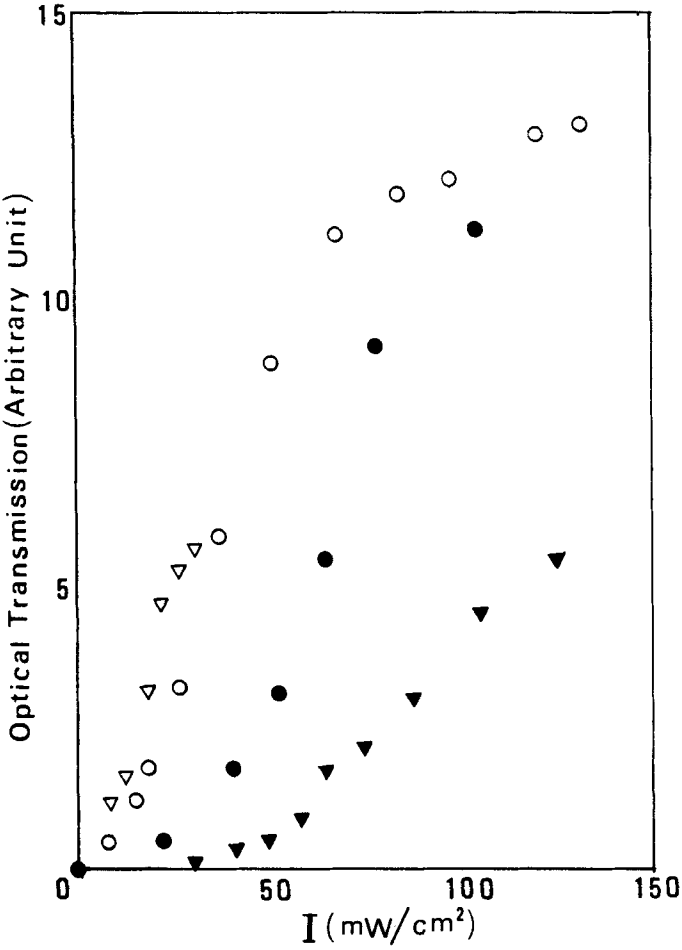

FIGURE 2 Variation in the optical transmission of homeotropic films as a function of the acoustic intensity. Individual curves are for the following frequencies: ●: 0.9 MHz, ○: 2.1 MHz, ▼: 3.1 MHz, ▽: 6.0 MHz.

The decay time τ_d, derived in the case of the electro-optic effect, is given as[6]

$$\frac{1}{\tau_d} = \frac{1}{\eta}\left(\frac{\Delta\varepsilon V^2}{4\pi L^2} - Kq^2\right) \tag{1}$$

where L is the layer thickness, η the viscosity coefficient and K the elastic constant. The wave number q is approximated by π/L. We fitted tentatively the experimental voltage dependence of τ_d, though rather scattered, to Eq. (1), and estimated η. The result gives $\eta = 6P$ at $I = 32$ mW/cm^2, where

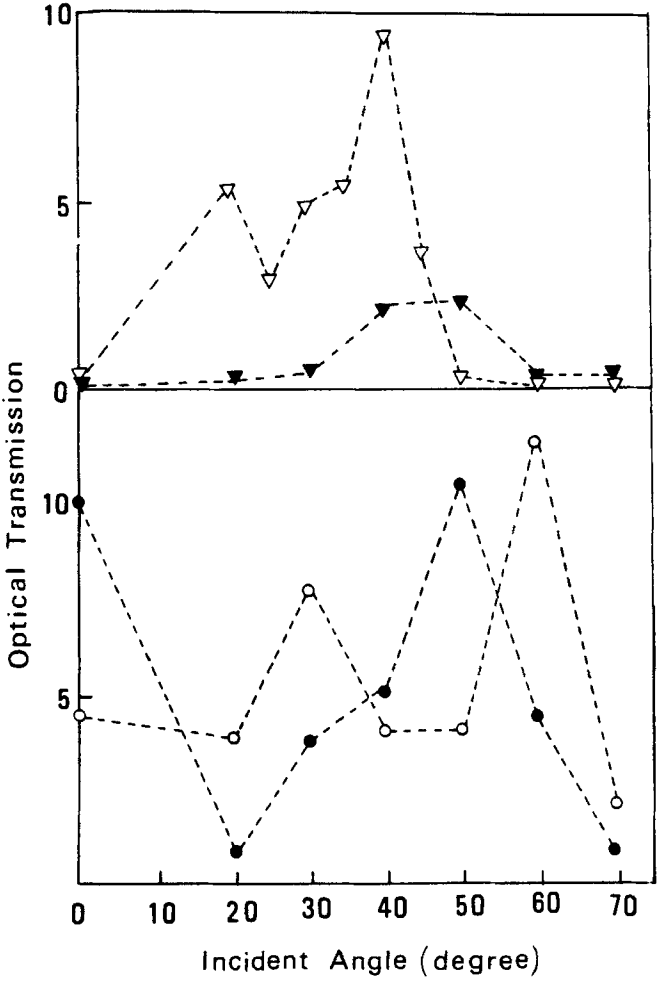

FIGURE 3 Angular dependence of the acousto-optical effect at the intensity of 30 mW/cm^2. The incident angle is defined as that between sound beam and the normal to the cell. Symbols are the same as in Figure 2.

$\Delta\varepsilon$ is put as $\Delta\varepsilon = 10$.[7] This value is 20 times larger than the capillary viscosity.[8] Moreover τ_d is strongly affected by the acoustic intensity. These discrepancies may be attributed to the fact that in Eq. (1) bulk fluid motion is ignored, while in our acoustic streaming model this effect is essential. The fluid motion leads to an apparent increase of the viscosity coefficient η.

Bertolotti *et al.*[9] and Bartoloni *et al.*[10] observed shorter response time at lower frequencies (their highest frequency is 200 KHz). This is presumably

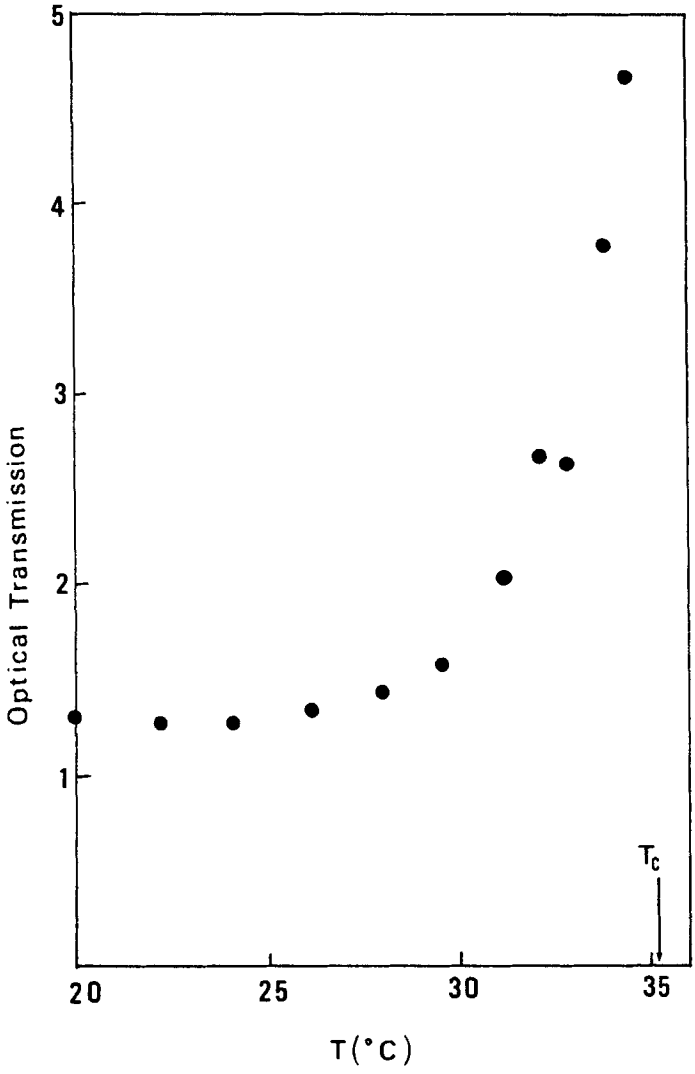

FIGURE 4 Temperature dependence of the acousto-optical effect at the intensity of 15 mW/cm^2. The transition temperature was 35.2°C. f = 2.1 MHz.

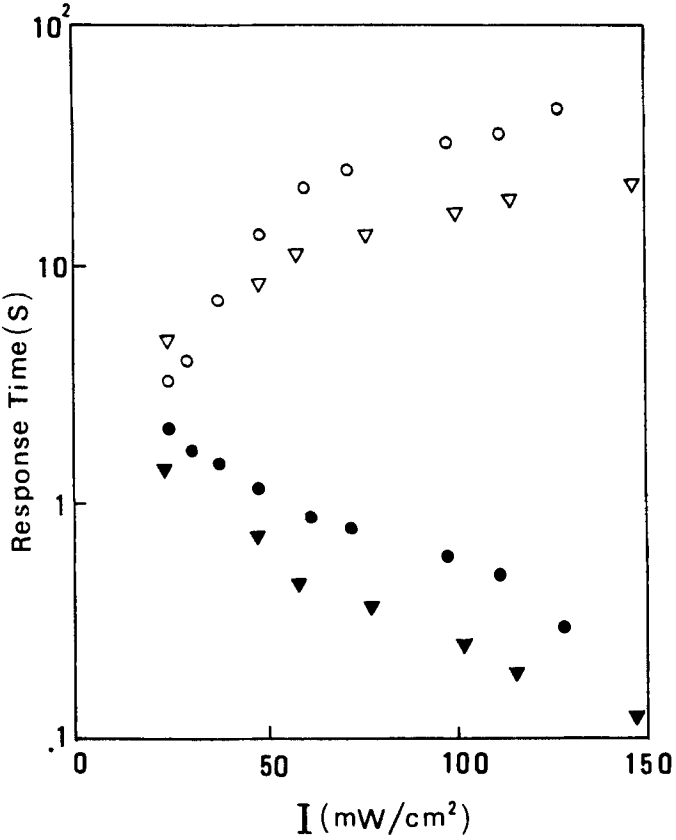

FIGURE 5 Rise and decay times as a function of the acoustic intensity. ●, ▼: rise time, ○, ▽: decay time. Filled and open triangles refer to the cell divided into small arrays. f = 2.1 MHz.

related to the first interaction between the director and the ultrasound, which is suppressed under our higher frequency conditions.

On the cell used in the above-mentioned work, however, clear ultrasonic images were not obtained. Non-irradiated regions also appeared bright. This observation indicates that the acoustic streaming will penetrate into the entire liquid crystal cell and smear out ultrasonic images.

3 IMPROVED LIQUID CRYSTAL IMAGE CONVERTER

Taking into account the before-mentioned features, we have made a liquid crystal image converter. Firstly in order to improve the resolution, the converter is divided into a matrix of small arrays, as illustrated in Figure 7.

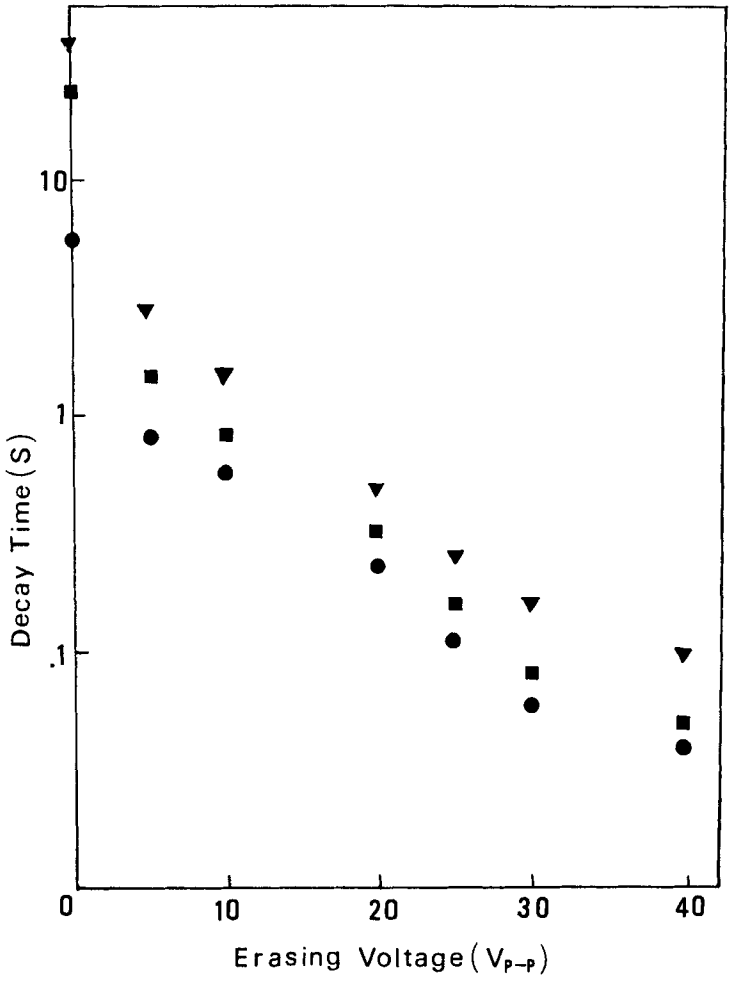

FIGURE 6 Decay time under an electric field. ●: I = 32 mW/cm^2, ■ : I = 61 mW/cm^2, ▼: I = 108 mW/cm^2. f = 2.1 MHz.

Photo resist film, RISTON (Dupont), was glued onto the glass plate. The film thickness was about 120 μm. The film was irradiated through a mask pattern with a mercury lamp and then unnecessary parts were removed. The cell was divided into small portions by stripes whose width is 0.1 mm and period is 1 mm. These dimensions were determined, considering the resolution $\sim\lambda$(λ is 0.75 mm at 2 MHz in PCB) together with simple fabrication. Stripes impede the acoustic streaming in arrays to interfere with each other and serve to keep the liquid crystal thickness constant. As the glass

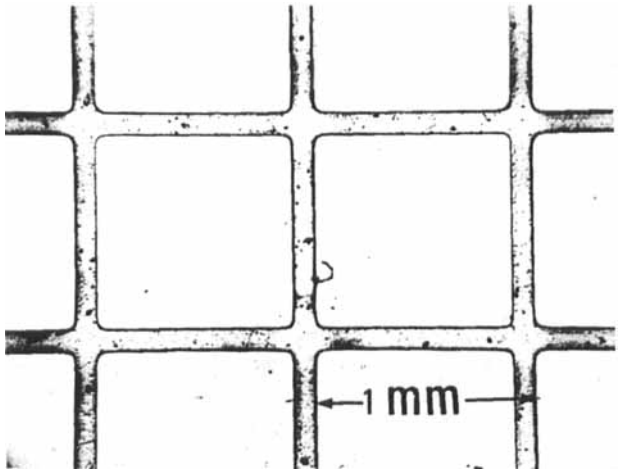

FIGURE 7 Photograph of the matrix.

plate is rather thin, it bends easily and the uniform thickness in a large area is not expected without the support of photo-resist film.

Secondly an erasing pulse was employed to reduce the decay time. The cell was irradiated with the pulsed ultrasound. During the turn-off interval of the ultrasound, the erasing pulse (100 Hz, 40 V_{p-p}) was applied to restore the initial orientation.

Experimental setup is depicted in Figure 8. Two successive pulse series are used. One is fed into an ultrasonic oscillator and the other drives a low

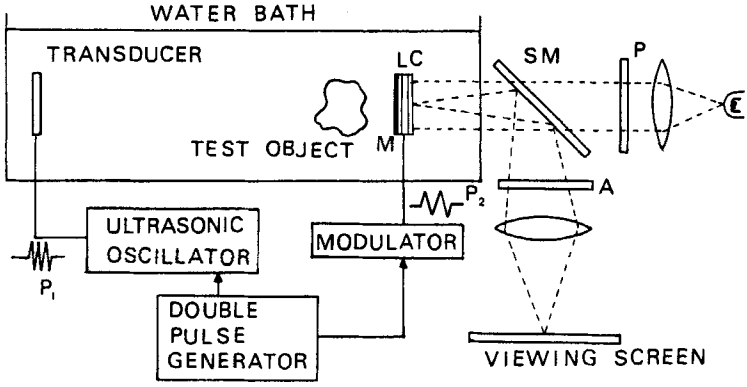

FIGURE 8 Schematic diagram of the experimental setup. P: polarizer, A: analyzer, SM: semi-transparent mirror, M: mirror of vaporized Al film, P_1: ultrasonic pulse, P_2: erasing pulse modulated at 100 Hz.

frequency modulator for erasing. The imaging light illuminates the surface of cell at the side opposite to the ultrasound. The reflected light is projected onto a view plane (mat glass).

Dividing of the cell into arrays does not affect the sensitivity. As shown in Figure 5, the response time is lessened to some extent. Since the acoustic streaming occurs within each small region of arrays of the cell, we think that it reaches up to a steady state and returns back to the initial state faster than the case of the non-divided cell.

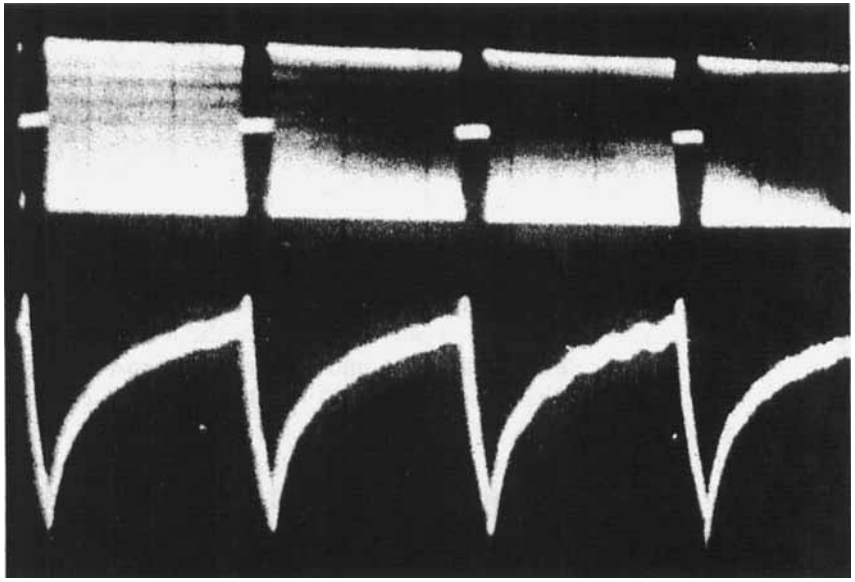

FIGURE 9 Optical transmission during the operation. The upper figure is the pulsed ultrasound and the lower the optical transmission of the cell. On removal of the ultrasound, erasing pulse is applied on the cell. 1 div = 0.2 s, $I = 70$ mW/cm^2, $f = 2.1$ MHz.

Figure 9 is the optical transmission during the operation. The direct transmission image of several objects, produced by placing them in contact with the cell, is shown in Figure 10. Compared with the previous results in Ref. 5, it is apparent that the image quality is significantly improved. Rather complicated objects are resolved. Under the best condition, the resolution exceeds the array dimension, attaining to about a half of that dimension.†

† The preliminary investigation showed that the more complete imaging system with an acoustic lens gave the same image quality.

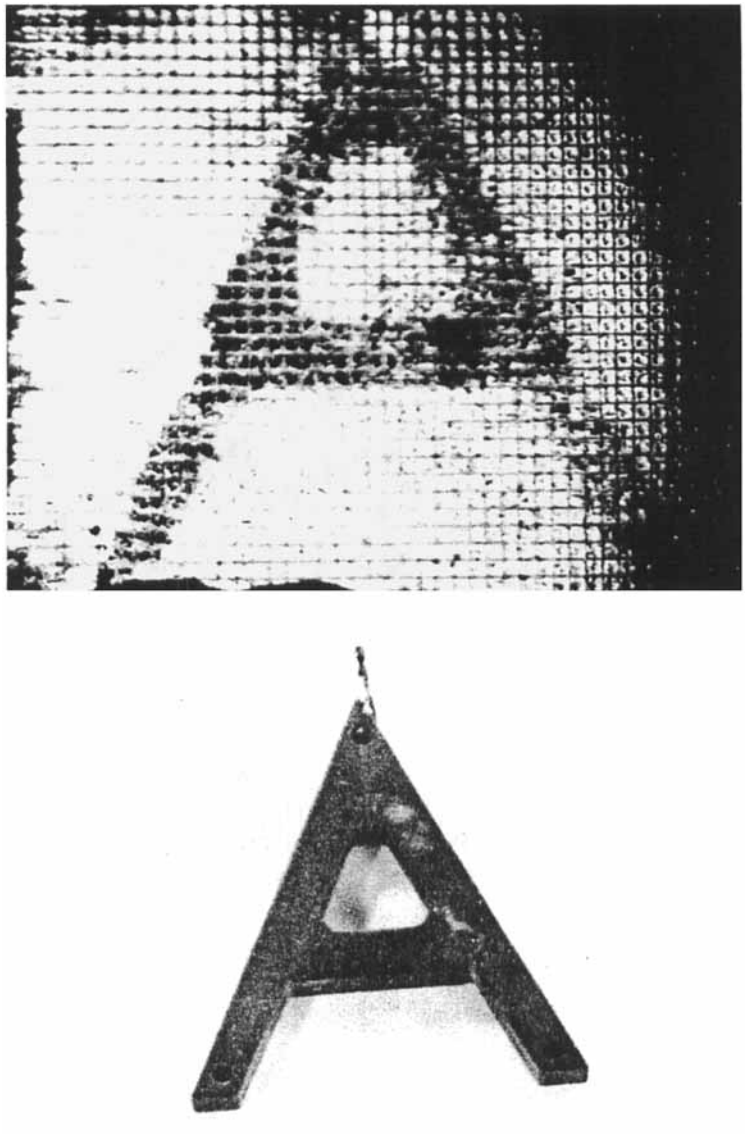

FIGURE 10 Test objects and their direct ultrasonic shadow images. (a) Letter A made of a brass plate (3 mm thick).

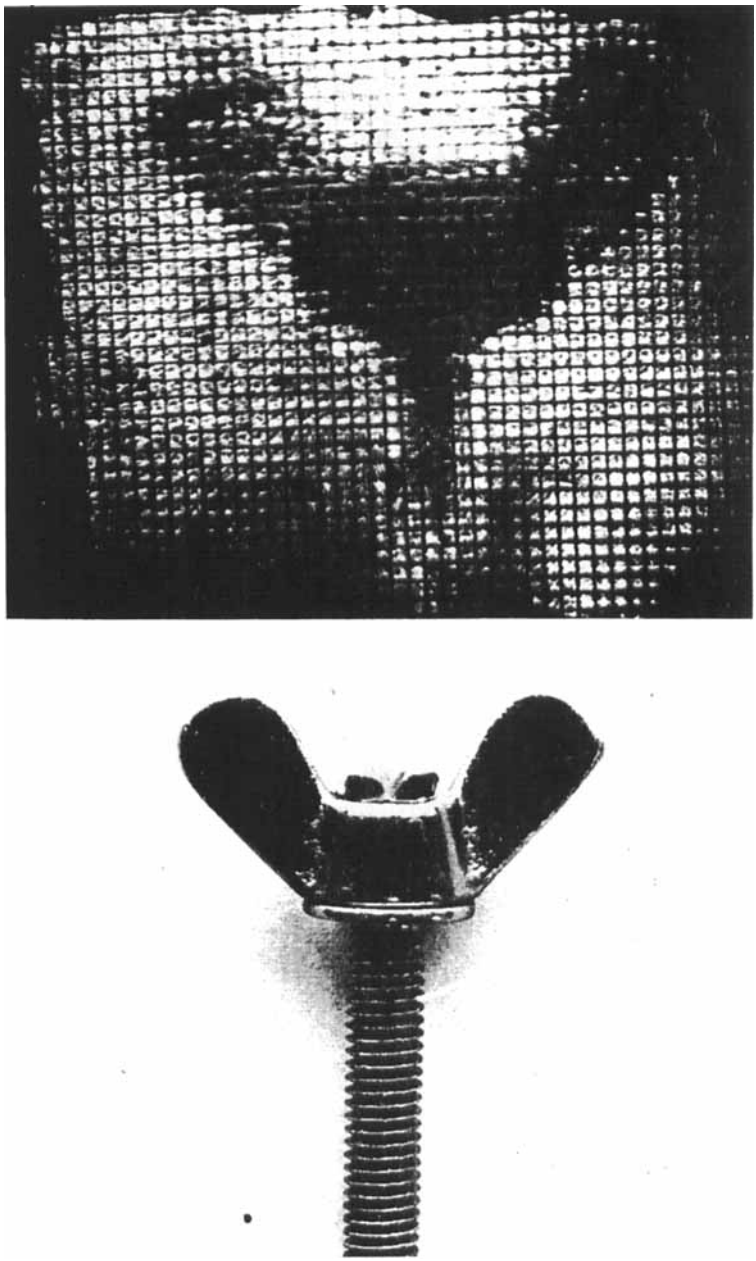

FIGURE 10 Test objects and their direct ultrasonic shadow images. (b) Top of a thumbscrew.

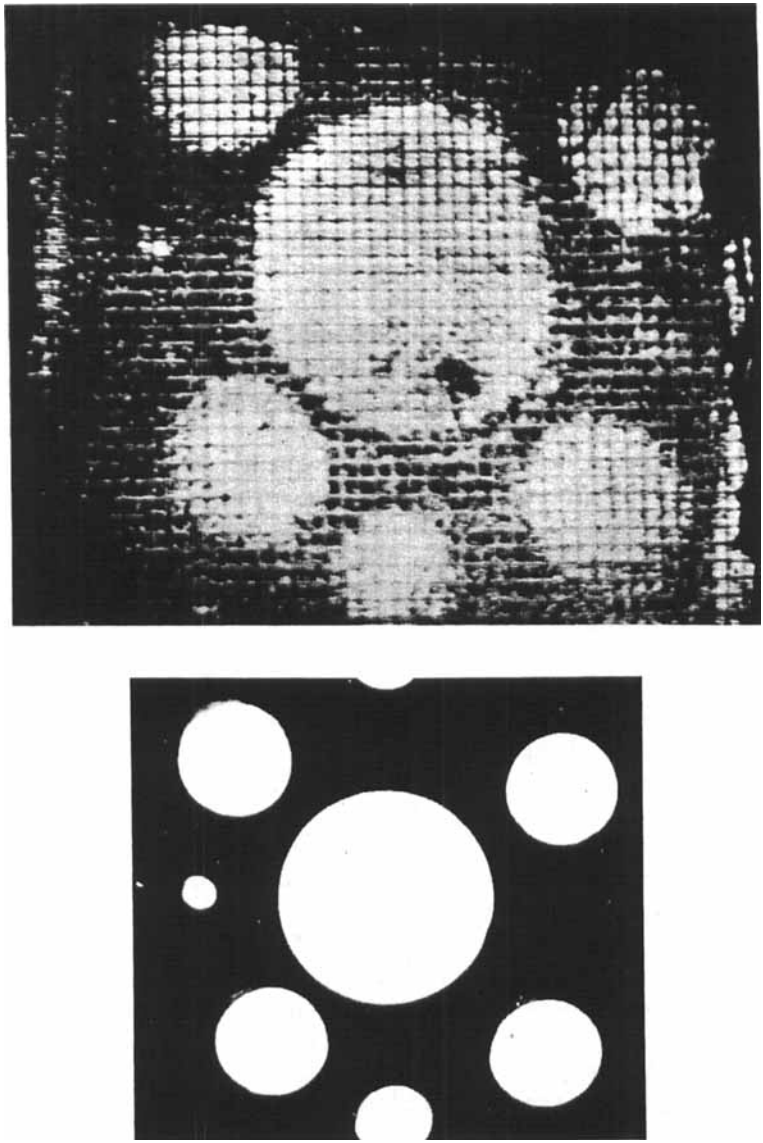

FIGURE 10 Test objects and their direct ultrasonic shadow images. (c) Perforated brass plate (3 mm thick). The objects were placed just in front of the cell. Photos were taken with an incandescent lamp. f = 2.1 MHz.

4 DISCUSSION

In this section we shall discuss the obtained results within the framework of the acoustic streaming model. In terms of the proposed mechanism, the optical transmission T_r is expressed as[5]

$$T_r = \frac{\alpha^2 I^2}{C^2} f(K_i, \alpha_i, L, a, b) \tag{2}$$

where I is the acoustic intensity, α the absorption constant, C the sound velocity. The function f contains as arguments Frank's elastic constants K_i, the viscosity coefficients α_i, L, a and b. $2a$ and $2b$ are the width of sound beam and the cell, respectively. Geometrical relations are shown in Figure 1. This function does not contain the ultrasonic frequency explicitly.

According to the above equation, the optical transmission is proportional to the square of the acoustic intensity. There is no threshold intensity, at which orientation changes abruptly. The frequency dependence is mainly determined by the absorption constant, which increases with increasing the ultrasonic frequency, provided that dispersion of other quantities could be neglected. Another factor affecting the optical transmission is the incident sound pattern. The sensitivity depends on the ratio a/b.

The results of Figure 2 were analyzed according to Eq. (2). In the range of the small optical transmission, as is shown in Figure 11, T_r varies as I^2, which agrees with the theory.

The frequency dependence was compared with the theory. The measured optical transmission changes in a complicated manner with the frequency and does not agree with Eq. (2). This is due to the multiple-reflection effect in the cell. The acoustic intensity in the cell is different from that measured in water. The acoustic intensity I_e effective to cause the streaming was evaluated in the case of normal ultrasonic incidence, assuming plane sound wave for simplicity (see appendix). This assumption is not exact as the actual sound field is not perfectly uniform, as is shown in Figure 12. However this discrepancy may not be serious for the discussion of the behaviour.

The optical transmission at the incident acoustic intensity of 30 mW/cm^2 was compared with Eq. (2). This nominal intensity is transformed to I_e according to the procedure described in the appendix. The values T_r/I_e^2 are plotted as a function of the ultrasonic frequency in Figure 13. The square of the absorption constant, which was determined previously[12] and would have the same frequency dependence, is also shown in this figure. The results agree with the relation predicted by the theory, though scattering to some extent.

It is difficult to discuss the temperature dependence of T_r. It might be partly explained from the behaviour of the absorption constant, which diverges near the transition temperature.

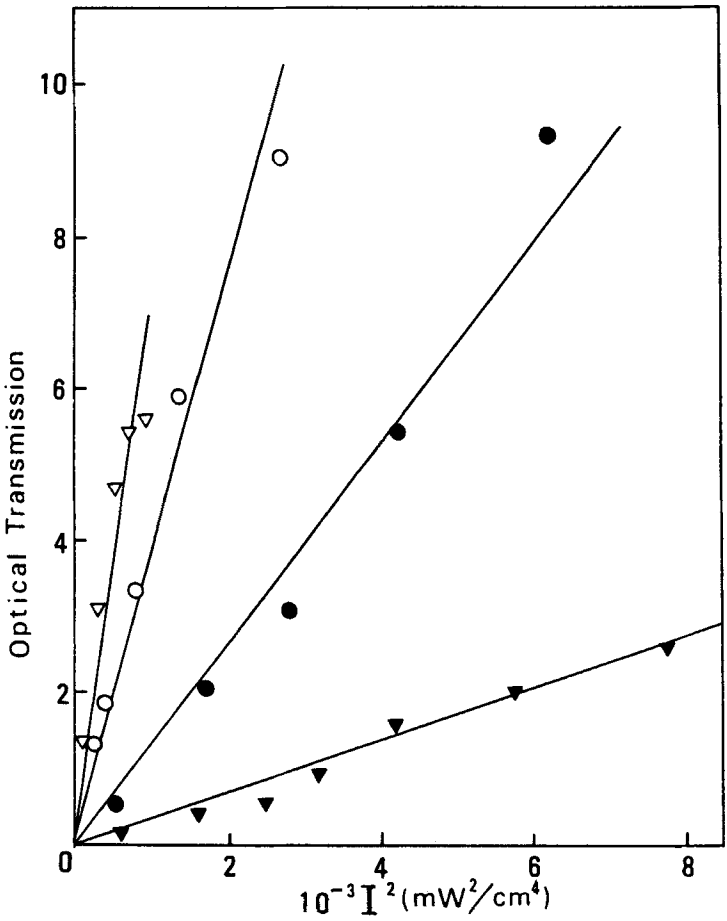

FIGURE 11 Plot of the optical transmission versus the square of the acoustic intensity. Symbols are the same as in Figure 2.

It may be mentioned that the apparent sensitivity would be increased by adjusting the thickness of the glass plate to $\lambda/2$. But this method is valid only near the normal incidence. Further, the thicker the glass plate is, the more the image quality deteriorates, because of the multiple-reflection effect in the cell. Eventually thin glass plates adopted by the authors transmit a considerable amount of the incident ultrasound and is less angle-dependent.

Recently Sripaipan *et al.*[13] proposed another model associated with the "horizontal" acoustic streaming effect. They have employed the cell whose two edges were left open. They assumed that at normal incidence the oscillating motion of the glass plate enduces waves to travel horizontally through

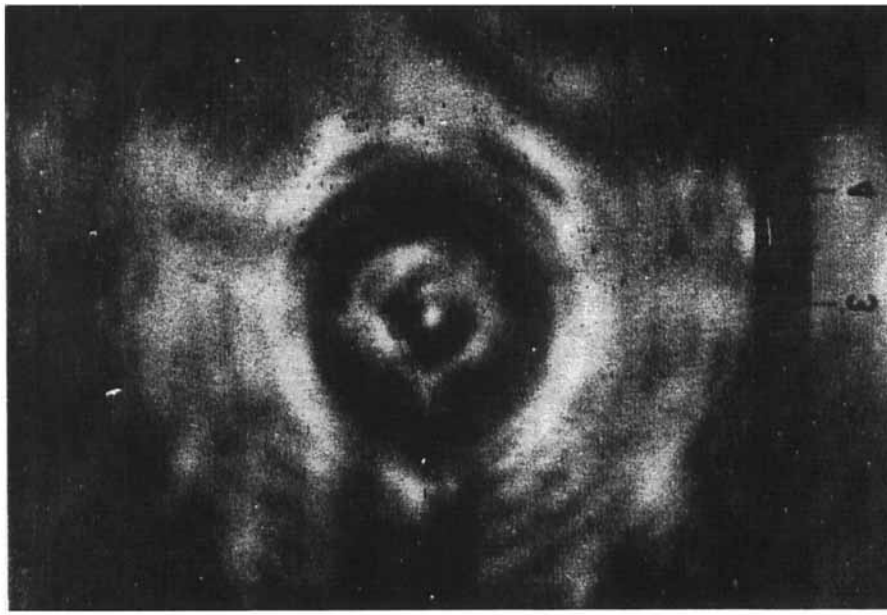

(a)

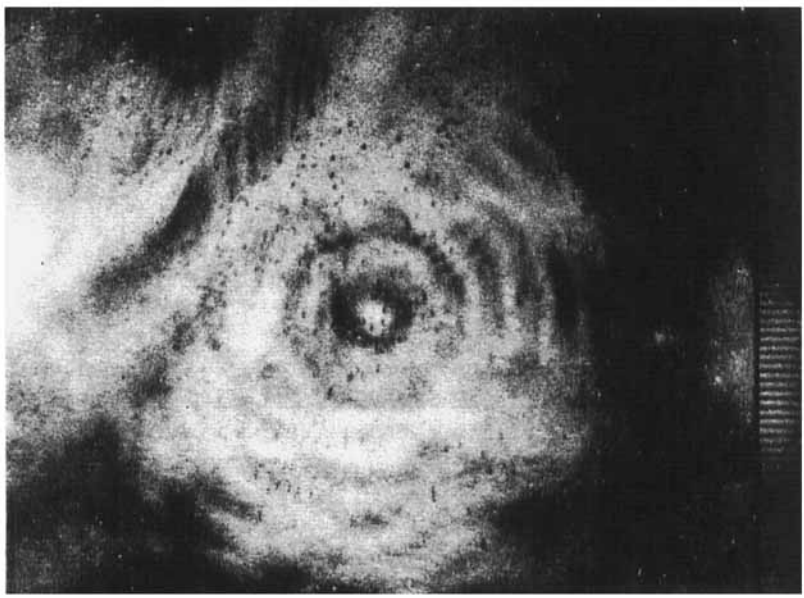

(b)

FIGURE 12 Actual sound field visualized by a Pohlman cell.[11] (a): $f = 3.1$ MHz, (b): $f = 2.1$ MHz.

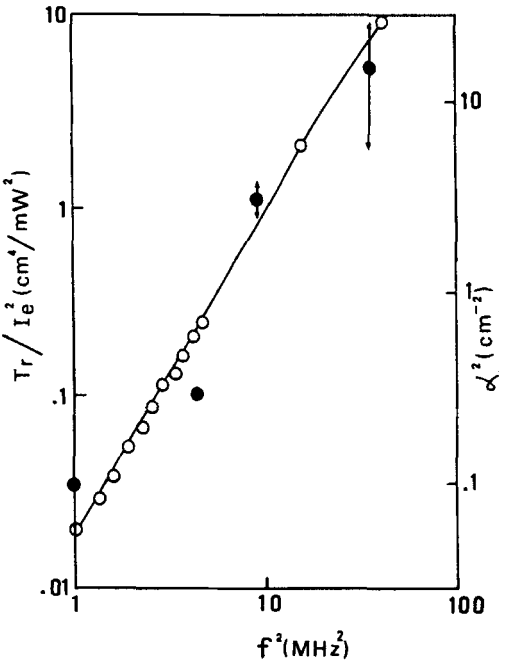

FIGURE 13 Plot of T_r/I_e^2 versus the ultrasonic frequency. The nominal acoustic intensity is 30 mW/cm^2, which is transformed to the effective intensity. Open circles show the values of α^2 at 25°C, measured with swept acoustical interferometry technique and pulse technique.[12]

the cell. Consequently, a standing wave may be set up between the air-liquid crystal boundaries with nodes and antinodes in line parallel to the boundaries. The standing wave causes the acoustic streaming between nodes and antinodes.[14]

We still feel that the acoustic streaming normal to the cell is mainly responsible for the acousto-optical effect in our experimental conditions, taking into account the following reasons.

1) We have used thin glass plates for the cell. Therefore, a large amount of sound wave transmits through the glass plates, sufficient to cause the acoustic streaming normal to the cell.

2) The orienting action of the ultrasound is also observed when the cell are irradiated at oblique incidence. In this case the horizontal standing wave is not expected, while our proposed streaming is still valid.

3) Furthermore, as shown in Figure 10, the cell whose period does not correspond to $nx\lambda/2$ (n:integer; The condition is required to form standing waves.) also appears birefringent.

In summary, our liquid crystal image converter is, at present, in a medium quality both in the response time and the image quality. But it needs no complicated electronics neither optics. Also, it can be easily extended to a detector with a larger area and could serve as a handy ultrasonic image detector.

Acknowledgements

The authors are indebted to Nippon Electric Co. for kindly fabricating a matrix of photo-resist.

References

1. L. Kessler and S. Sawyer, *Appl. Phys. Lett.*, **17**, 440 (1970).
2. H. Mailer, K. Likins, T. Taylor and J. Fergason, *Appl. Phys. Lett.*, **18**, 105 (1971).
3. P. Greguss, *Acoustica*, **29**, 52 (1973).
4. P. Greguss, Ultrasonics International 1975. Conference Proceedings, p. 195.
5. S. Nagai, A. Peters, and S. Candau, *Rev. Phys. Appl.* (Paris), **12**, 21 (1977).
6. E. Jakeman and E. P. Raynes, *Phys. Lett.*, **A39**, 69 (1972).
7. G. W. Gray, K. J. Harrison, and J. A. Nash, *Electron. Lett.*, **9**, 130 (1973).
8. F. Kiry and P. Martinoty, *J. Phys.* (*Paris*), **38**, 153 (1977).
9. M. Bertolotti, S. Matellucci, F. Scudieri, and D. Sette, *Appl. Phys. Lett.*, **24**, 74 (1972).
10. R. Bartolino, M. Bertolotti, F. Scudieri, D. Sette, and A. Sliwinski, *J. Appl. Phys.*, **46**, 1928 (1975).
11. B. P. Hildebrand and B. B. Brenden, "An Introduction to Acoustical Holography" (Plenum Press New York, 1972), p. 162.
12. S. Nagai, P. Martinoty, and S. Candau, *J. Phys.* (Paris), **37**, 769 (1976).
13. C. Sripaipan, C. F. Hayes, and G. T. Fang, *Phys. Rev.*, **A15**, 1297 (1977).
14. W. L. Nyborg, "Physical Acoustics," Vol II ed. by W. P. Mason (Academic Press, New York, 1965).
15. W. T. Thomson, *J. Appl. Phys.*, **21**, 89 (1950).
16. L. Q. Spielvogel, *J. Appl. Phys.*, **42**, 3667 (1971).

Appendix

The liquid crystal cell consists of glass-liquid crystal-glass layers. The incident acoustic intensity is different from that in liquid crystal layer. The effective intensity is estimated as follows:

The transmission of plane sound wave through a multi-layered cell is expressed[15,16] (see Figure 14)

$$\begin{pmatrix} P_{K+1} \\ U_{K+1} \end{pmatrix} = \begin{pmatrix} \cos \Delta_{K.K+1} & -i\rho_K C_K \sin \Delta_{K.K+1} \\ -\dfrac{i}{\rho_K C_K} \sin \Delta_{K.K+1} & \cos \Delta_{K.K+1} \end{pmatrix} \begin{pmatrix} P_K \\ U_K \end{pmatrix} \quad (1')$$

$$\Delta_{K.K+1} = \frac{2\pi L_{K.K+1}}{\lambda_{K.K+1}}$$

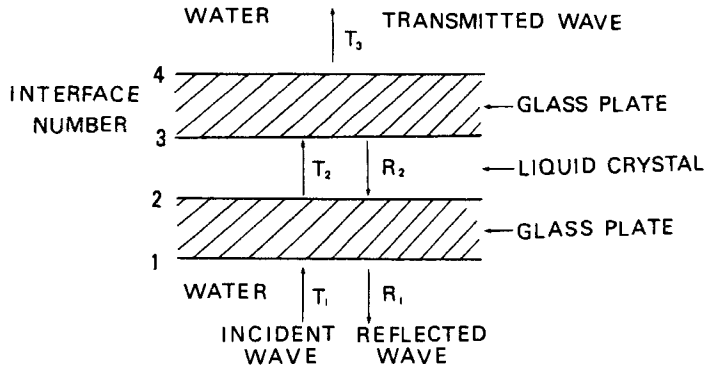

FIGURE 14 Ultrasonic transmission through a liquid crystal cell.

where subscript index K refers to interface number. P_K and U_K are the sound pressure and the particle velocity. $\lambda_{K.K+1}$ is the wavelength. $L_{K.K+1}$ the thickness of the layer. Equation (1′) is applied recursively across adjacent layers to obtain the final transmitted wave.

Knowing the relation between the incident and transmitted wave, the progressive and reflected wave amplitudes, T and R, in each layer are given

$$\begin{aligned} T &= \tfrac{1}{2}(P + U\rho C) \\ R &= \tfrac{1}{2}(P - U\rho C) \end{aligned} \tag{2′}$$

The acoustic intensity effective to cause the acoustic streaming in liquid crystals is defined as the difference of two components.

$$I_e = \frac{(|T_2|^2 - |R_2|^2)}{|T_1|^2} I_{\text{incident}} \tag{3′}$$

The following values were used for numerical evaluation. $\rho_{\text{water}} = \rho_{LC} = 1$ g/cm^3, $\rho_{\text{glass}} = 2.8$ g/cm^3, $C_{\text{water}} = C_{LC} = 1.5 \times 10^5$ cm/s, $C_{\text{glass}} = 5.8 \times 10^5$ cm/s.